Eur Biophys J (2012) 41:437–448
DOI 10.1007/s00249-012-0797-5

ORIGINAL PAPER

EBSA
Biophysics in Europe

Kinetic and mesoscopic non-equilibrium description of the Ca^{2+} pump: a comparison

Anders Lervik · Dick Bedeaux · Signe Kjelstrup

Received: 25 October 2011 / Revised: 31 January 2012 / Accepted: 29 February 2012 / Published online: 28 March 2012

Abstract We analyse the operation of the Ca^{2+}-ATPase ion pump using a kinetic cycle diagram. Using the methodology of Hill, we obtain the cycle fluxes, entropy production and efficiency of the pump. We compare these results with a mesoscopic non-equilibrium description of the pump and show that the kinetic and mesoscopic pictures are in accordance with each other. This gives further support to the mesoscopic theory, which is less restricted and also can include the heat flux as a variable. We also show how motors can be characterised in terms of unidirectional backward fluxes. We proceed to show how the mesoscopic approach can be used to identify fast and slow steps of the model in terms of activation energies, and how this can be used to simplify the kinetic diagram.

Keywords Ca^{2+}-ATPase · Active transport · Ion pump · Kinetic model · Mesoscopic model

Introduction

The lipid bilayers of biological membranes are generally impermeable to ions and most polar molecules (a notable exception being osmosis of water) and represent a physical barrier to transport (Berg et al. 2002; Nelson 2003). Integral membrane proteins may act as pumps and channels and enable transport of ions and molecules essential for cell operation across the membrane with high selectivity (Berg et al. 2002; Nelson 2003; Garrett and Grisham 2010).

Among the transporting integral membrane proteins are the P-type ATPases, which actively transport cations across biological membranes. The P-type ATPases constitute a large family of membrane proteins including the Ca^{2+}-ATPase, the Na^+/K^+-ATPase, the plant and fungal H^+-ATPases and the heavy-metal-transporting ATPases (Møller et al. 2010; Kühlbrandt 2004; Lee and East 2001). The sarcoplasmic reticulum Ca^{2+}-ATPase (SERCA) was the first of the P-type ATPases for which a 3D structure was determined by Toyoshima et al. (2000). The structure of the Ca^{2+}-ATPase in one of its conformations is shown in Fig. 1. Since the first 3D structure was reported, several other conformations[1] of Ca^{2+}-ATPase have also been resolved (Xu et al. 2002; Toyoshima and Nomura 2002; Sørensen et al. 2004; Olesen et al. 2004, 2007a; Toyoshima and Mizutani 2004; Toyoshima et al. 2004, 2007, 2011; Obara et al. 2005; Søhoel et al. 2006; Jensen et al. 2006; Moncoq et al. 2007; Takahashi et al. 2007; Laursen et al. 2009; Winther et al. 2010), enabling a structural interpretation of the operation of the pump. Combined with the vast experimental kinetic and mutagenic data available for the Ca^{2+}-ATPase, this has led to a detailed picture of the

A. Lervik (✉) · D. Bedeaux · S. Kjelstrup
Department of Chemistry, Norwegian University of Science and Technology, Trondheim, Norway
e-mail: anders.lervik@chem.ntnu.no

D. Bedeaux
e-mail: dick.bedeaux@chem.ntnu.no

S. Kjelstrup
e-mail: signe.kjelstrup@chem.ntnu.no

S. Kjelstrup
Process and Energy Laboratory, Delft University of Technology, Delft, The Netherlands

[1] Forty-five structures have been deposited in the Protein Data Bank, with the identification codes 1FQU, 1IWO, 1KJU, 1SU4, 1T5S, 1T5T, 1VFP, 1WPE, 1WPG, 1XP5, 2AGV, 2BY4, 2C88, 2C8K, 2C8L, 2C9M, 2DQS, 2EAR, 2EAS, 2EAT, 2EAU, 2O9J, 2OA0, 2Z9R, 2ZBD, 2ZBE, 2ZBF, 2ZBG, 3AR2, 3AR3, 3AR4, 3AR5, 3AR6, 3AR7, 3AR8, 3AR9, 3B9B, 3B9R, 3BA6, 3FGO, 3FPB, 3FPS, 3NAL, 3NAM and 3NAN.

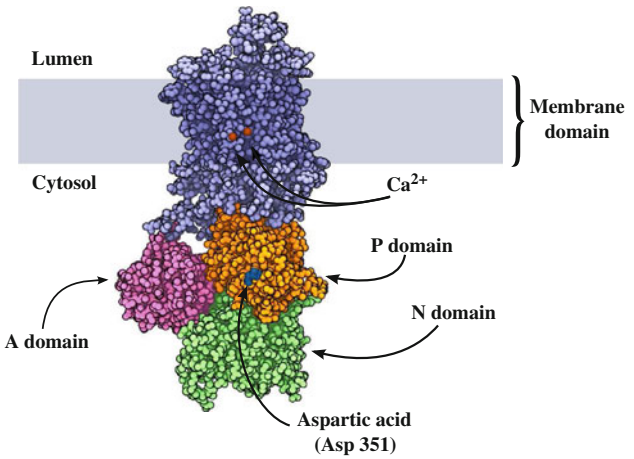

Fig. 1 Structure of the Ca^{2+}-ATPase in the E1 conformation with bound calcium ions (entry 1T5T in the Protein Data Bank) (Sørensen et al. 2004). The calcium ions are coloured *dark orange*, the actuator (A) domain is coloured *pink*, the nucleotide binding (N) domain is coloured *green* and the phosphorylation (P) domain is coloured *orange*. The aspartic acid residue (Asp351) which is phosphorylated during the operation of the pump is coloured *dark blue*. The transmembrane part of the protein consists of 10 α-helices, coloured *light blue*

transport cycle, and positioned the pump as a prototype for the P-type ATPases (Møller et al. 2010; Kühlbrandt 2004).

Mathematical modelling of the pump pre-dates the recent determination of the structures by several decades. The pump was discovered in the 1960s (Hasselbach and Makinose 1961; Schatzmann 1966), and several models for the pump cycle have since been proposed, ranging from simple kinetic models with few states (Kanazawa et al. 1971; Mintz and Guillain 1997) to more elaborate and complex kinetic models (Froud and Lee 1986; Gould et al. 1986; McWhirter et al. 1987; Haynes and Mandveno 1987; Alonso et al. 2001). Generally, these models describe the pump cycle according to a Post–Albers scheme (Apell 2004) in terms of two conformations, E1 and E2, where E1 has high affinity for Ca^{2+} and E2 has high affinity for protons (Møller et al. 2010; Apell 2004). A minimal description of the pump cycle begins with the binding of Ca^{2+} ions from the cytosol to the E1 state and phosphorylation by ATP, resulting in an occluded state. Following the phosphorylation is a conformational change to an occluded E2 state, with subsequent luminal opening of the transmembrane region of the protein and release of the Ca^{2+} ions to the lumen. The protein is then dephosphorylated and returns to the E1 state. Concomitant with the binding/release of Ca^{2+} is release/binding of two or three H^+ ions (Møller et al. 2010).

The models based on the Post–Albers scheme are able to capture many of the features of the pump. However, they generally focus on the kinetic properties, disregarding thermodynamics. A notable exception is the model of active transport developed by Smith and Crampin (2004) for the Na^+/K^+-ATPase and applied to the Ca^{2+}-ATPase by Tran et al. (2009). This model incorporates thermodynamics by considering detailed balance at equilibrium, which results in a thermodynamic constraint for the rate constants (Tran et al. 2009). However, the ability to model heat transfer is lacking in all the kinetic models. Several studies have shown that the calcium pump is able to transport heat (Kodama et al. 1982; de Meis et al. 1997; de Meis 2001a, b, 2002, 2003; Barata and de Meis 2002; Arruda et al. 2003; Kjelstrup et al. 2008) and that the pump might contribute to non-shivering thermogenesis (de Meis et al. 2005; Mall et al. 2006; Mahmmoud 2008). In order to address these points, Bedeaux, Kjelstrup and others (Kjelstrup et al. 2005a, b; Bedeaux and Kjelstrup 2008; Kjelstrup et al. 2009) applied the theory of mesoscopic non-equilibrium thermodynamics and derived equations that describe the active ion transport and the accompanying heat transport. This represents a thermodynamic basis for the theoretical description of the pump. Such a basis has thus an advantage, and the method should therefore be further substantiated.

In this paper we show how the kinetic and thermodynamic description of cycle reactions are connected, and use this connection to compare the kinetic and thermodynamic description of the cycle operation of the Ca^{2+}-ATPase. We also compare the cycle descriptions with the mesoscopic non-equilibrium thermodynamic (MNET) model of Bedeaux and Kjelstrup (2008).

We present the kinetic model and analyse it according to the methodology of Hill (1989) in "Kinetic model" and obtain the flux of calcium ions and reaction rate. Following this, we perform the mesoscopic analysis of the same model in "Mesoscopic thermodynamic model" and obtain the fluxes in this framework. Subsequently, we compare the different models with the aforementioned MNET model of Bedeaux and Kjelstrup, and find that they are all compatible for isothermal conditions.

Kinetic model

We will consider a kinetic model based on the recent six-state model of Møller et al. (2010) proposed on the basis of the determined 3D structures of the pump and reproduced here in Fig. 2.

For the kinetic modelling we introduce the possibility of slip by considering a transition between two of the states as shown in Fig. 3. On traversing the cycle in the positive direction, the following steps occur: From state A to state B, two Ca^{2+} ions are exchanged with n protons ($n = 2-3$), concurrent with a conformational change (E2 to E1). On moving from state B to C, ATP is hydrolysed, resulting in

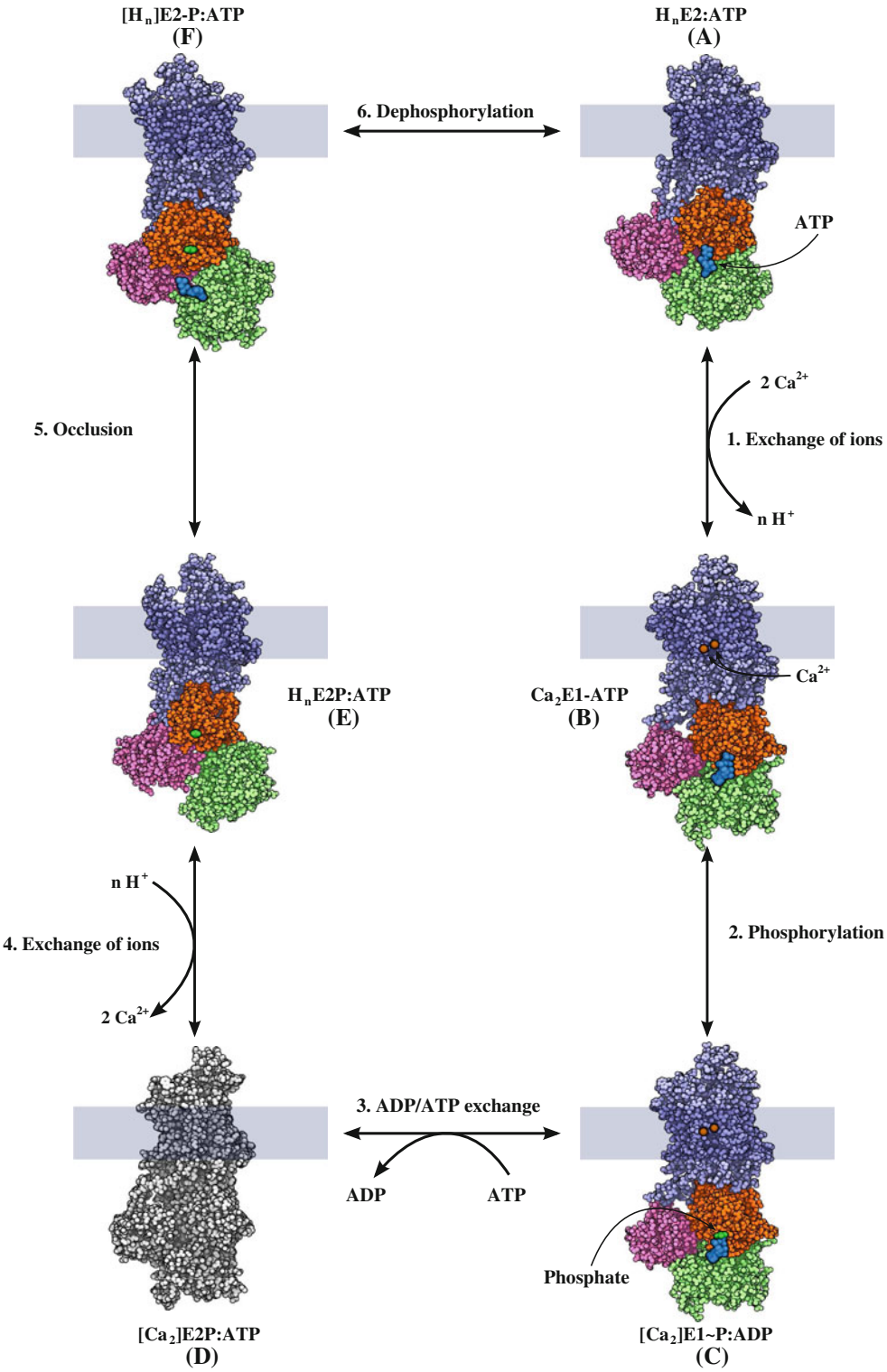

Fig. 2 The transport cycle of SERCA 1a, in terms of the key states, adapted from Møller et al. (2010). In this adoption the states are also labelled A,B,…,F as shown. The calcium ions are coloured *dark orange*, the actuator (A) domain is coloured *pink*, the nucleotide binding (N) domain is coloured *green* and the phosphorylation (P) domain is coloured *orange*. ATP/ADP is coloured *light blue*, while the phosphate group is coloured *green*. The 3D structure of the D-state has not yet been obtained and is represented here by the Ca_2E1P phosphoenzyme intermediate, PDB accession code: 3BA6 (Olesen et al. 2007b), coloured *grey*

an occluded state, and subsequently (C to D), ADP is exchanged with ATP while the enzyme returns to the E2 conformation. In the next step (D to E), de-occlusion occurs with exchange of bound Ca^{2+} ions with n protons ($n = 2-3$) from the lumen. The bound protons are then occluded (E to F) before the cycle is completed by dephosphorylation (F to A). In state D the pump can also move directly to state B by dephosphorylation. This results in a kinetic diagram consisting of three cycles, labelled a, b and c as shown in Fig. 4. Cycle a is equivalent to a non-slip cycle, and cycle b is the hydrolysis of ATP, represented by (Alberty and Goldberg 1992; Alberty 2003)

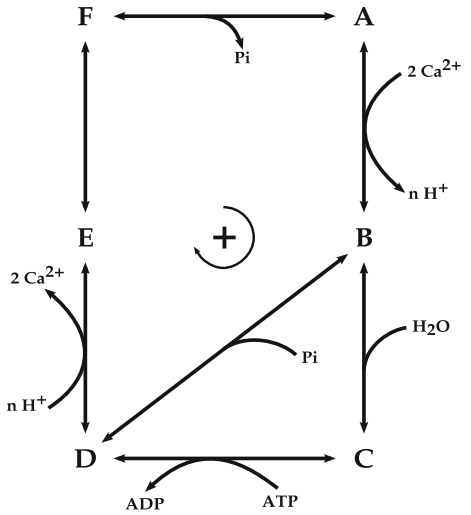

Fig. 3 Kinetic diagram for the operation of the ATPase. On traversing the cycle in the positive direction, one ATP molecule is hydrolysed and two Ca^{2+} ions are moved to the luminal side, concurrent with transport of n H^+ ions in the opposite direction. ATP or ADP is bound to the enzyme in all the states. The states denoted A–F in the diagram are the states H_nE2:ATP, Ca_2E1:ATP, $[Ca_2]E1P$:ADP, $[Ca_2]E2P$:*ATP*, H_nE2P:ATP and $[H_n]E2$:ATP, respectively, using the notation of Møller et al. (2010), where square brackets denote an occluded state. Slip (excess energy dissipation) is introduced by considering the possibility of direct transition between the states B and D. Between states B and C we have added binding of water which participates in the ATP hydrolysis

$$\mathrm{ATP} + \mathrm{H_2O} \rightleftharpoons \mathrm{ADP} + \mathrm{P_i}, \tag{1}$$

where ATP, ADP and P_i are the sum of species of adenosine triphosphate, adenosine diphosphate and inorganic phosphate, respectively. At 298 K, pH = 7.0, 10 mM $MgCl_2$ P_i = 10 mM and $[ATP]/[ADP] = 10^3$, the reaction Gibbs energy is −57 kJ mol^{-1} (Bedeaux and Kjelstrup 2008). The third cycle, c, is the exchange of ions between the cytosol and lumen. The pump can attain a concentration difference corresponding to a 20−40,000 ratio of the concentrations in the lumen and cytosol (Møller et al. 2010). At 298 K, these concentration ratios correspond to a Gibbs energy of exchanging two calcium ions from the cytosol to the lumen of approximately 49–53 kJ mol^{-1}. Combining this with the Gibbs energy of the ATP hydrolysis, the net change in Gibbs energy is negative and the pump cycles in the forward direction, moving calcium ions from the cytosol to the lumen at the expense of ATP hydrolysis. For the case of a positive net change in Gibbs energy, the pump will cycle in the negative direction and synthesize ATP molecules, using the energy stored in the concentration gradient.

Hill (1989), with later extensions (Qian 2005, 2007, 2009), devised a framework for analysing kinetic cycles, and following this methodology, we introduce the probabilities P_j of the enzyme being in state j and the (pseudo-)first-order

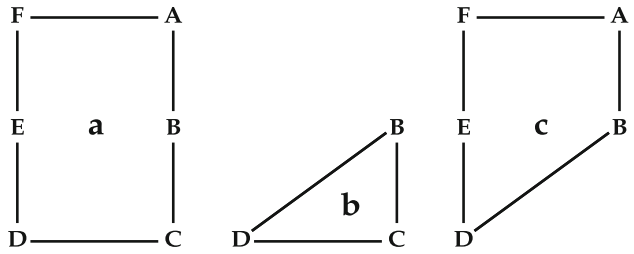

Fig. 4 The three cycles of the slipping kinetic model of the operation of the pump. The three cycles are labelled a, b and c, respectively. The replacement of cycle a by cycles b and c implies that the strict coupling in a is loosened

rate constants k_{ij} for the transition from state $i \rightarrow$ state j. Transitions involving the binding of a component are also treated as a first-order process: If the transition $m \rightarrow n$ involves the binding of a component, say S, the rate constant for the transition can be defined in terms of a second-order rate constant, k^*_{mn}, and the concentration, c_S, of the binding component: $k_{mn} = k^*_{mn} c_S$; For example, ATP is bound to the enzyme in transition between states C and D in the kinetic diagram (Fig. 3) and $k_{CD} = k^*_{CD} c_{ATP}$.

The rate of change of the probabilities can be found from the kinetic diagram,

$$\begin{aligned}
\frac{\mathrm{d}P_A}{\mathrm{d}t} &= (-k_{AB}P_A + k_{BA}P_B) + (k_{FA}P_F - k_{AF}P_A) \\
&= -J_{AB} + J_{FA}, \\
\frac{\mathrm{d}P_B}{\mathrm{d}t} &= (k_{AB}P_A - k_{BA}P_B) - (k_{BC}P_B - k_{CB}P_C) \\
&\quad - (k_{BD}P_B - k_{DB}P_D) = J_{AB} - J_{BC} - J_{BD}, \\
&\vdots \\
\frac{\mathrm{d}P_F}{\mathrm{d}t} &= (-k_{FA}P_F + k_{AF}P_A) + (k_{EF}P_E - k_{FE}P_F) \\
&= -J_{FA} + J_{EF},
\end{aligned} \tag{2}$$

where $J_{ij} = k_{ij}P_i - k_{ji}P_j$ is the net transition flux from $i \rightarrow j$, and the normalization condition is

$$P_A + P_B + P_C + P_D + P_E + P_F = 1. \tag{3}$$

In the steady state, $\mathrm{d}P_j/\mathrm{d}t = 0$, and Eqs. 2 and 3 can be solved (for instance using Cramer's rule) in terms of the probabilities P_j, and the transition fluxes can be obtained.

Alternatively, the transition fluxes can also be expressed in terms of the cycle fluxes in the steady state, J_a, J_b and J_c,

$$\begin{aligned}
J_{AB} &= J_{DE} = J_{EF} = J_{FA} = J_a + J_c, \\
J_{BC} &= J_{CD} = J_a + J_b, \\
J_{BD} &= J_c - J_b,
\end{aligned} \tag{4}$$

which shows that there are two independent transition fluxes in steady state, and that the cycle fluxes cannot be determined from the transition fluxes alone. However, as shown by Hill (1989), the cycle fluxes can be obtained by

$$J_a = \frac{(\Pi_{a+} - \Pi_{a-})\sum_a}{\sum}, \quad J_b = \frac{(\Pi_{b+} - \Pi_{b-})\sum_b}{\sum}, \quad J_c = \frac{(\Pi_{c+} - \Pi_{c-})\sum_c}{\sum}, \tag{5}$$

where

$$\begin{aligned}
\Pi_{a+} &= k_{AB}k_{BC}k_{CD}k_{DE}k_{EF}k_{FA},\\
\Pi_{a-} &= k_{AF}k_{FE}k_{ED}k_{DC}k_{CB}k_{BA},\\
\Pi_{b+} &= k_{BC}k_{CD}k_{DB},\\
\Pi_{b-} &= k_{BD}k_{DC}k_{CB},\\
\Pi_{c+} &= k_{AB}k_{BD}k_{DE}k_{EF}k_{FA},\\
\Pi_{c-} &= k_{AF}k_{FE}k_{ED}k_{DB}k_{BA},
\end{aligned} \tag{6}$$

and $\sum$, $\sum_a$, $\sum_b$ and $\sum_c$ are obtained using the diagram method (Hill 1989) (we show in "Appendix" how the terms in $\sum$ can be obtained). Specifically,

$$\begin{aligned}
\sum &= k_{FA}k_{EF}k_{DE}k_{CD}k_{BA} + k_{FA}k_{EF}k_{DE}k_{CB}k_{BD}\\
&\quad + 82\,\text{other terms},\\
\sum\nolimits_a &= 1,\\
\sum\nolimits_b &= k_{AB}k_{EF}k_{FA} + k_{AF}k_{FE}k_{ED}\\
&\quad + k_{AB}k_{FE}k_{ED} + k_{AB}k_{ED}k_{FA},\\
\sum\nolimits_c &= k_{CB} + k_{CD}.
\end{aligned} \tag{7}$$

Detailed balance gives

$$\begin{aligned}
\frac{\Pi_{a+}}{\Pi_{a-}} &= K_{eq}\frac{c_{H_2O}c_{ATP}}{c_{ADP}c_{Pi}}\left(\frac{c^{cyt}_{Ca^{2+}}}{c^{lum}_{Ca^{2+}}}\right)^2\left(\frac{c^{lum}_{H^+}}{c^{cyt}_{H^+}}\right)^4\\
&= \exp\left(\frac{X_r}{RT}\right)\left[\exp\left(\frac{X_{Ca/2H}}{RT}\right)\right]^2 = \exp\left(\frac{X_a}{RT}\right),\\
\frac{\Pi_{b+}}{\Pi_{b-}} &= K_{eq}\frac{c_{H_2O}c_{ATP}}{c_{ADP}c_{Pi}} = \exp\left(\frac{X_r}{RT}\right) = \exp\left(\frac{X_b}{RT}\right),\\
\frac{\Pi_{c+}}{\Pi_{c-}} &= \left(\frac{c^{cyt}_{Ca^{2+}}}{c^{lum}_{Ca^{2+}}}\right)^2\left(\frac{c^{lum}_{H^+}}{c^{cyt}_{H^+}}\right)^4 = \left[\exp\left(\frac{X_{Ca/2H}}{RT}\right)\right]^2\\
&= \exp\left(\frac{X_c}{RT}\right),
\end{aligned} \tag{8}$$

which defines the cycle forces (X_a, X_b and X_c) in terms of the thermodynamic forces (X_r and $X_{Ca/2H}$),

$$\begin{aligned}
X_r &= \mu_{ATP} + \mu_{H_2O} - \mu_{Pi} - \mu_{ADP} = -\Delta_r G,\\
X_{Ca/2H} &= \left(\mu^{cyt}_{Ca^{2+}} - 2\mu^{cyt}_{H^+}\right) - \left(\mu^{lum}_{Ca^{2+}} - 2\mu^{lum}_{H^+}\right)\\
&= \mu^{cyt}_{Ca/2H} - \mu^{lum}_{Ca/2H} = -\Delta\mu_{Ca/2H},
\end{aligned} \tag{9}$$

where c_i is the concentration of species i, $\Delta_r G$ is the Gibbs energy of the ATP hydrolysis, K_{eq} is the corresponding equilibrium constant and $\Delta\mu_{Ca/2H}$ is the change in Gibbs energy on moving one calcium ion from the cytosol to the lumen and two protons in the opposite direction. The superscripts "cyt" and "lum" refers to the concentrations in the cytosol and lumen, respectively. Here we assume that the exchange of calcium with protons is electroneutral (i.e. two protons are exchanged per calcium ion). As argued by Bedeaux and Kjelstrup (2008), net charge build-up is unlikely in absence of redox reactions, and in addition, there can be leak pathways for protons. Tran et al. (2009) argued that the formation of a steady-state H^+ gradient is unlikely since the sarcoplasmic reticulum vesicle membrane is highly permeable to protons. In our case, the contribution of the H^+ ions to the thermodynamic force would then be negligible. For completeness, this contribution is retained in the following development.

The flux of calcium ions can be found from the cycle fluxes as

$$\begin{aligned}
\frac{J_{Ca}}{2} &= J_a + J_c = \frac{\Pi_{a+} - \Pi_{a-}}{\sum} + \frac{(\Pi_{c+} - \Pi_{c-})\sum_c}{\sum}\\
&= \frac{\Pi_{a-}}{\sum}\left(\frac{\Pi_{a+}}{\Pi_{a-}} - 1\right) + \frac{\Pi_{c-}\sum_c}{\sum}\left(\frac{\Pi_{c+}}{\Pi_{c-}} - 1\right),\\
&= J_{a-}\left(\exp\left(\frac{X_r}{RT}\right)\left[\exp\left(\frac{X_{Ca/2H}}{RT}\right)\right]^2 - 1\right)\\
&\quad + J_{c-}\left(\left[\exp\left(\frac{X_{Ca/2H}}{RT}\right)\right]^2 - 1\right),
\end{aligned} \tag{10}$$

where $J_{j^-} = \Pi_{j-}\Sigma_j/\Sigma$ is the one-way cycle flux in the negative (backward) direction for cycle j and the power of 2 accounts for transport of two calcium ions per cycle. Similarly, the reaction rate is

$$\begin{aligned}
r &= J_a + J_b = \frac{\Pi_{a+} - \Pi_{a-}}{\sum} + \frac{(\Pi_{b+} - \Pi_{b-})\sum_b}{\sum}\\
&= \frac{\Pi_{a-}}{\sum}\left(\frac{\Pi_{a+}}{\Pi_{a-}} - 1\right) + \frac{\Pi_{b-}\sum_b}{\sum}\left(\frac{\Pi_{b+}}{\Pi_{b-}} - 1\right),\\
&= J_{a-}\left(\exp\left(\frac{X_r}{RT}\right)\left[\exp\left(\frac{X_{Ca/2H}}{RT}\right)\right]^2 - 1\right)\\
&\quad + J_{b-}\left(\exp\left(\frac{X_r}{RT}\right) - 1\right).
\end{aligned} \tag{11}$$

For small values of the thermodynamic forces, $|X_r + 2X_{Ca/2H}| \ll RT$, we expand the exponentials and obtain the flux of calcium ions as

$$\begin{aligned}
\frac{J_{Ca}}{2} &= J_{a-}\left(\frac{X_r}{RT} + 2\frac{X_{Ca/2H}}{RT}\right) + 2J_{c-}\frac{X_{Ca/2H}}{RT}\\
&= J_{a-}\frac{X_r}{RT} + 2(J_{a-} + J_{c-})\frac{X_{Ca/2H}}{RT},\\
J_{Ca} &= -D^0_{dr}\frac{\Delta_r G}{RT} - D^0_{dd}\frac{\Delta\mu_{Ca/2H}}{RT},
\end{aligned} \tag{12}$$

where $D^0_{dr} = 2J_{a-}$ and $D^0_{dd} = 4(J_{a-} + J_{c-})$. The reaction rate for the same conditions is

$$
\begin{aligned}
r &= J_{a-}\left(\frac{X_r}{RT} + 2\frac{X_{Ca/2H}}{RT}\right) + J_{b-}\frac{X_r}{RT} \\
&= 2J_{a-}\frac{X_{Ca/2H}}{RT} + (J_{a-} + J_{b-})\frac{X_r}{RT}, \\
r &= -D^0_{rd}\frac{\Delta\mu_{Ca/2H}}{RT} - D^0_{rr}\frac{\Delta_r G}{RT},
\end{aligned}
\tag{13}
$$

where $D^0_{rd} = 2J_{a-}$ and $D^0_{rr} = J_{a-} + J_{b-}$. These relations give interpretations of diffusion coefficients (Onsager coefficients) in terms of backward-directed unidirectional cycle fluxes (Hill 1982). These should be characteristic for each motor and could be used to compare functions. Such fluxes are obtainable from radioisotope studies.

Since the one-way cycle fluxes are positive,

$$
\begin{aligned}
&D^0_{dr} = D^0_{rd} \geq 0, \qquad && D^0_{dd}/2 \geq D^0_{rd}, \\
&D^0_{dr} \leq 2D^0_{rr}, && \left(D^0_{rd}\right)^2 \leq D^0_{rr}D^0_{dd}.
\end{aligned}
\tag{14}
$$

For comparison, Bedeaux and Kjelstrup (Bedeaux and Kjelstrup 2008; Kjelstrup et al. 2009) gave the following expression for the flux of calcium ions and reaction rate near global equilibrium (adapted to an isothermal case):

$$
\begin{aligned}
J_{Ca} &= -D^0_{dr}\frac{\Delta_r G}{RT} - D^0_{dd}\frac{\Delta\mu_{Ca/2H}}{RT}, \\
r &= -D^0_{rr}\frac{\Delta_r G}{RT} - D^0_{rd}\frac{\Delta\mu_{Ca/2H}}{RT}
\end{aligned}
\tag{15}
$$

and the following relations for the coefficients for a stoichiometric pump (when $J_{Ca}/r = 2$),

$$
D_{dd}/2 = D_{rd}, \quad D_{dr} = 2D_{rr}, \tag{16}
$$

which are reproduced here for a stoichiometric pump which has $J_{b-} = 0$ and $J_{c-} = 0$.

The dissipation of energy is given by the cycle fluxes and forces (Hill 1989)

$$
\begin{aligned}
T\sigma &= J_a X_a + J_b X_b + J_c X_c \\
&= J_a\left(X_r + 2X_{Ca/2H}\right) + J_b X_r + 2J_c X_{Ca/2H} \\
&= (J_a + J_b)X_r + 2(J_a + J_c)X_{Ca/2H} \\
&= rX_r + J_{Ca}X_{Ca/2H}, \\
\sigma &= -r\frac{\Delta_r G}{T} - J_{Ca}\frac{\Delta\mu_{Ca/2H}}{T},
\end{aligned}
\tag{17}
$$

where σ is the entropy production. The efficiency for pumping, η, can be defined by (Hill 1989; Qian 2009)

$$
\begin{aligned}
\eta &= \frac{W_{ideal} - W_{lost}}{W_{ideal}} = \frac{J_{Ca}\left(-X_{Ca/2H}\right)}{r \cdot X_r} \\
&= \frac{-2(J_a + J_c)X_{Ca/2H}}{(J_a + J_b)X_r},
\end{aligned}
\tag{18}
$$

where W_{ideal} is the maximum obtainable work and the lost work, W_{lost}, can be obtained from the Gouy–Stodola theorem, $W_{lost} = T\sigma$. This expression is no ad hoc definition but has its base in a second-law analysis, exergy analysis and non-equilibrium thermodynamics. It applies to microscopic systems as long as the assumption of local equilibrium applies (Kjelstrup and Bedeaux 2008). The expression is equivalent to that proposed by Qian et al. (2008) for the thermodynamic efficiency. Possible viscous dissipation, see e.g. Qian et al. (2008), makes the term $T\sigma$ larger by adding one more flux and force to the dissipation (Kjelstrup et al. 2010).

A negative J_c and a positive J_b flux decrease the efficiency. Using the previously stated values for the Gibbs energy of the ATP hydrolysis and the exchange of calcium ions we see that $J_a > 0$, $J_b > 0$ and $J_c < 0$, and this lowers the efficiency of the pump as expected. In this case, the stoichiometry is not necessarily equal to 2; however, this is recovered if $J_b = 0$ and $J_c = 0$, which corresponds to a non-slip (stoichiometric) case. Also, the inequalities in Eq. 14 reduce to equalities in the non-slip case. At equilibrium, the reversible pump has $\eta = 1$ and $\sigma = 0$ and the fluxes are zero.

Mesoscopic thermodynamic model

Having obtained the fluxes and forces for the operation of the pump using the kinetic description, we now analyse the pump in the framework of mesoscopic non-equilibrium thermodynamics. Subsequently, we will compare the obtained fluxes and forces with previously derived relations for operation of the pump (Bedeaux and Kjelstrup 2008).

Analysis of the reaction cycle

A reaction cycle can be analysed within the framework of mesoscopic non-equilibrium thermodynamics. In the mesoscopic description, the reaction cycle is analysed on a more detailed scale by introducing the reaction coordinates, γ_{ij}, as additional variables (Kjelstrup et al. 2005a). For the kinetic model given in Fig. 3, the coordinates are γ_{ij} with $ij = \mathrm{AB}, \mathrm{BC}, \ldots, \mathrm{FA}$ and $ij = \mathrm{BD}$. The diffusion, J_{ij}, along the reaction coordinate γ_{ij} is given by

$$
\begin{aligned}
J_{ij}(\gamma_{ij}, t) = -D_{ij}\exp\left(\frac{-\Phi_{ij}(\gamma_{ij})}{RT}\right) \\
\times \frac{\partial}{\partial\gamma_{ij}}\exp\left(\frac{\mu_{ij}(\gamma_{ij}, t)}{RT}\right),
\end{aligned}
\tag{19}
$$

where D_{ij} is the diffusion coefficient, Φ_{ij} is the potential through which the diffusion process takes place, and μ_{ij} is the chemical potential,

$$
\mu_{ij}(\gamma_{ij}, t) = RT\ln P_{ij}(\gamma_{ij}, t) + \Phi_{ij}(\gamma_{ij}), \tag{20}
$$

where P_{ij} is the probability of state γ_{ij}.

The activation energy for the overall process is large, of order 80–90 kJ/mol (Peinelt and Apell 2004, 2005). The fluxes can therefore be treated as quasi-stationary, $J_{ij}(\gamma_{ij}, t) = J_{ij}(t)$. For constant diffusion coefficients, Eq. 19 can be integrated to

$$J_{ij}(t) = -\frac{D_{ij}}{\int \mathrm{d}\gamma_{\mathrm{ij}} \exp\left(\Phi_{\mathrm{ij}}(\gamma_{\mathrm{ij}})/\mathrm{RT}\right)} \times \left[\exp\left(\frac{\mu_{ij}(1,t)}{RT}\right) - \exp\left(\frac{\mu_{ij}(0,t)}{RT}\right)\right]. \tag{21}$$

The boundary conditions for the chemical potentials can be found from Fig. 3 as

$$\begin{aligned}
&\mu_{\mathrm{AB}}(0) = \mu_{\mathrm{A}} + 2\mu^{\mathrm{cyt}}_{\mathrm{Ca^{2+}}}, && \mu_{\mathrm{AB}}(1) = \mu_{\mathrm{B}} + 4\mu^{\mathrm{cyt}}_{\mathrm{H^{+}}},\\
&\mu_{\mathrm{BC}}(0) = \mu_{\mathrm{B}} + \mu_{\mathrm{H_2O}}, && \mu_{\mathrm{BC}}(1) = \mu_{\mathrm{C}},\\
&\mu_{\mathrm{CD}}(0) = \mu_{\mathrm{C}} + \mu_{\mathrm{ATP}}, && \mu_{\mathrm{CD}}(1) = \mu_{\mathrm{D}} + \mu_{\mathrm{ADP}},\\
&\mu_{\mathrm{DE}}(0) = \mu_{\mathrm{D}} + 4\mu^{\mathrm{lum}}_{\mathrm{H^{+}}}, && \mu_{\mathrm{DE}}(1) = \mu_{\mathrm{E}} + 2\mu^{\mathrm{lum}}_{\mathrm{Ca^{2+}}},\\
&\mu_{\mathrm{EF}}(0) = \mu_{\mathrm{E}}, && \mu_{\mathrm{EF}}(1) = \mu_{\mathrm{F}},\\
&\mu_{\mathrm{FA}}(0) = \mu_{\mathrm{F}}, && \mu_{\mathrm{FA}}(1) = \mu_{\mathrm{A}} + \mu_{\mathrm{Pi}},\\
&\mu_{\mathrm{BD}}(0) = \mu_{\mathrm{B}} + \mu_{\mathrm{Pi}}, && \mu_{\mathrm{BD}}(1) = \mu_{\mathrm{D}},
\end{aligned} \tag{22}$$

where the explicit time dependence has been suppressed. We note that the change in Gibbs energy for each cycle can be found by summing the Gibbs energy differences, $\Delta G_{ij} = \mu_{ij}(1) - \mu_{ij}(0)$, for each coordinate γ_{ij} in the cycle. This gives

$$\begin{aligned}
&\Delta G_{\mathrm{a}} = \Delta G_{\mathrm{b}} + \Delta G_{\mathrm{c}} = -X_{\mathrm{a}},\\
&\Delta G_{\mathrm{b}} = \Delta_{\mathrm{r}} G = -X_{\mathrm{b}}, \quad \Delta G_{\mathrm{c}} = 2\Delta\mu_{\mathrm{Ca/2H}} = -X_{\mathrm{c}},
\end{aligned} \tag{23}$$

where ΔG_k is the change in Gibbs energy for cycle k in the positive direction.

Using

$$\frac{P_j}{P_j^{\mathrm{eq}}} = \exp\left(\frac{\mu_j - \mu_j^{\mathrm{eq}}}{RT}\right), \tag{24}$$

with $\mu_i^{\mathrm{eq}} = \mu_j^{\mathrm{eq}}$, the normalization condition in Eq. 3 can be rewritten as

$$\sum_{j=\{\mathrm{A},\ldots,\mathrm{F}\}} P_j^{\mathrm{eq}} \exp\left(\frac{\mu_j - \mu_j^{\mathrm{eq}}}{RT}\right) = 1. \tag{25}$$

Together with the steady-state relations from Eq. 2, the different transition fluxes can then be obtained using Cramer's rule.

For the case of no slip (when γ_{BD} and the corresponding boundary conditions are not included), all the obtained fluxes are equal and

$$J_{\mathrm{AB}} = \frac{D}{\sum'}\left(\left[\exp\left(\frac{X_{\mathrm{Ca/2H}}}{RT}\right)\right]^2 \exp\left(\frac{X_{\mathrm{r}}}{RT}\right) - 1\right), \tag{26}$$

with $D = D_{\mathrm{AB}}D_{\mathrm{BC}}D_{\mathrm{CD}}D_{\mathrm{DE}}D_{\mathrm{EF}}D_{\mathrm{FA}}$ and $\sum'$ is a collection of terms not shown here. The flux of calcium ions and the reaction rate can be obtained by $J_{\mathrm{Ca}} = 2J_{\mathrm{AB}}$ and $r = J_{\mathrm{AB}}$. This corresponds to Eqs. 10 and 11 for the case $J_{\mathrm{b}\pm} = 0$ and $J_{\mathrm{c}\pm} = 0$.

For the case with slip, two of the obtained transition fluxes are independent in accordance with Eq. 4, and one obtains (for instance)

$$J_{\mathrm{AB}} = \frac{D'}{\sum''}\left(\left[\exp\left(\frac{X_{\mathrm{Ca/2H}}}{RT}\right)\right]^2 - 1\right) + \frac{D''}{\sum''}\left(\left[\exp\left(\frac{X_{\mathrm{Ca/2H}}}{RT}\right)\right]^2 \exp\left(\frac{X_{\mathrm{r}}}{RT}\right) - 1\right) \tag{27}$$

and

$$J_{\mathrm{BC}} = \frac{D^*}{\sum''}\left(\exp\left(\frac{X_{\mathrm{r}}}{RT}\right) - 1\right) + \frac{D^{**}}{\sum''}\left(\left[\exp\left(\frac{X_{\mathrm{Ca/2H}}}{RT}\right)\right]^2 \exp\left(\frac{X_{\mathrm{r}}}{RT}\right) - 1\right), \tag{28}$$

where the explicit forms of D', D'', D^*, D^{**} and $\sum''$ are not shown here. However, one can show that the equality $D'' = D^{**}$, is satisfied in this case. The flux of calcium ions and the reaction rate can be obtained by $J_{\mathrm{Ca}} = 2J_{\mathrm{AB}}$ and $r = J_{\mathrm{BC}}$.

The transition fluxes obtained in the mesoscopic framework have the same form as the fluxes obtained in the kinetic framework. The connection can be made more explicit by considering the flux in the kinetic description, $J_{ij} = k_{ij}P_i - k_{ji}P_j$, which can be written as (using detailed balance)

$$\begin{aligned}
J_{ij} &= k_{ij}P_i^{\mathrm{eq}}\left(\frac{P_i}{P_i^{\mathrm{eq}}} - \frac{P_j}{P_j^{\mathrm{eq}}}\right)\\
&= k_{ij}P_i^{\mathrm{eq}} \exp\left(-\frac{\mu_i^{\mathrm{eq}}}{RT}\right)\left[\exp\left(\frac{\mu_i}{RT}\right) - \exp\left(\frac{\mu_j}{RT}\right)\right].
\end{aligned} \tag{29}$$

Equations 21 and 29 relate the kinetic parameters to the diffusion coefficients and activation energies, for instance,

$$k_{\mathrm{EF}}P_{\mathrm{E}}^{\mathrm{eq}} = \frac{D_{\mathrm{EF}} \exp(\mu_{\mathrm{E}}^{\mathrm{eq}}/RT)}{\int \mathrm{d}\gamma_{\mathrm{EF}} \exp(\Phi_{\mathrm{EF}}(\gamma_{\mathrm{EF}})/RT)}. \tag{30}$$

This shows the equivalence of the kinetic and mesoscopic description of the cycle model.

Before comparing the different models, we note that the relations between the kinetic coefficients and the activation energy for the diffusion process can be used to identify the slow and fast steps of the model. The activation energies for the direct transition between states B and D, the ATP

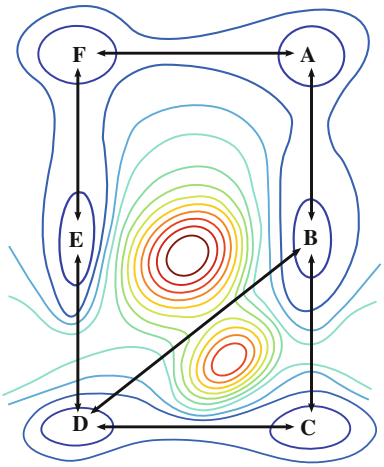

Fig. 5 Illustration of an activation energy landscape corresponding to the six-state kinetic diagram, leading to a possible reduction to a two-state description. The contour lines representing the energy landscape are drawn from low values (*blue colour*) to high values (*red colour*). There are high barriers between states B and D, states B and C and states D and E, but not between states D and C. This leads to essentially two states, X and Y

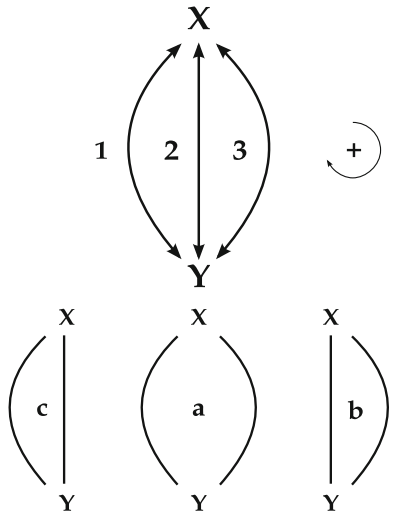

Fig. 6 The two-state kinetic diagram for the operation of the ATPase. The binding of the different species are not shown explicitly. The three cycles of the diagram are labelled a, b and c, corresponding to the three cycles in the original diagram. The three paths between the two states are labelled 1–3 (from *left* to *right*)

hydrolysis (states B and C) and the exchange of bound calcium with hydrogen ions in the lumen (states D to E) is large. This is depicted in Fig. 5. The six-state diagram can then be reduced to a two-state diagram, in terms of the states X and Y, as shown in Fig. 6 by assuming equilibrium between states A, B, E and F and states C and D. The probabilities of being in the two states X and Y are given by

$$P_{\mathrm{X}} = P_{\mathrm{A}} + P_{\mathrm{B}} + P_{\mathrm{E}} + P_{\mathrm{F}}, \quad P_{\mathrm{Y}} = P_{\mathrm{C}} + P_{\mathrm{D}}. \tag{31}$$

Further, the transitions $i \to j$ between the states are described with kinetic coefficients $\alpha_{ij,l}$ where l labels the path between the states. The kinetic coefficients $\alpha_{ij,l}$ can be obtained in terms of the original coefficients, and one may show that

$$\begin{aligned}
\frac{\Pi_{\mathrm{a}+}}{\Pi_{\mathrm{a}-}} &= \frac{\alpha_{\mathrm{XY},3}\alpha_{\mathrm{YX},1}}{\alpha_{\mathrm{XY},1}\alpha_{\mathrm{YX},3}} = \frac{k_{\mathrm{AB}}k_{\mathrm{BC}}k_{\mathrm{CD}}k_{\mathrm{DE}}k_{\mathrm{EF}}k_{\mathrm{FA}}}{k_{\mathrm{AF}}k_{\mathrm{FE}}k_{\mathrm{ED}}k_{\mathrm{DC}}k_{\mathrm{CB}}k_{\mathrm{BA}}}, \\
\frac{\Pi_{\mathrm{b}+}}{\Pi_{\mathrm{b}-}} &= \frac{\alpha_{\mathrm{XY},3}\alpha_{\mathrm{YX},2}}{\alpha_{\mathrm{YX},3}\alpha_{\mathrm{XY},2}} = \frac{k_{\mathrm{CD}}k_{\mathrm{DB}}k_{\mathrm{BC}}}{k_{\mathrm{DC}}k_{\mathrm{CB}}k_{\mathrm{BD}}}, \\
\frac{\Pi_{\mathrm{c}+}}{\Pi_{\mathrm{c}-}} &= \frac{\alpha_{\mathrm{XY},2}\alpha_{\mathrm{YX},1}}{\alpha_{\mathrm{YX},2}\alpha_{\mathrm{XY},1}} = \frac{k_{\mathrm{AB}}k_{\mathrm{BD}}k_{\mathrm{DE}}k_{\mathrm{EF}}k_{\mathrm{FA}}}{k_{\mathrm{AF}}k_{\mathrm{FE}}k_{\mathrm{ED}}k_{\mathrm{DB}}k_{\mathrm{BA}}},
\end{aligned} \tag{32}$$

which is identical to the relations given in Eq. 6. Continuing the analysis for the two-state model, we then obtain the same fluxes and forces as in the six-state model.

Contracted description

The flux of calcium ions and rate of reaction are of the same form in the two (kinetic and mesoscopic) cycle models. Bedeaux and Kjelstrup (2008) derived relations for the operation of the pump using MNET without making reference to a specific cycle model. These relations also apply to a non-isothermal case and include the heat flux. For a isothermal case the flux of calcium ions and the reaction rate are (Bedeaux and Kjelstrup 2008)

$$\begin{aligned}
J_{\mathrm{Ca}} &= -D_{\mathrm{dr}}\left[1 - \exp\left(-\frac{\Delta_{\mathrm{r}}G}{RT}\right)\right] \\
&\quad + D_{\mathrm{dd}}\left[1 - \exp\left(\frac{\Delta\mu_{\mathrm{Ca/2H}}}{RT}\right)\right], \\
r &= -D_{\mathrm{rr}}\left[1 - \exp\left(-\frac{\Delta_{\mathrm{r}}G}{RT}\right)\right] \\
&\quad + D_{\mathrm{rd}}\left[1 - \exp\left(\frac{\Delta\mu_{\mathrm{Ca/2H}}}{RT}\right)\right].
\end{aligned} \tag{33}$$

For brevity, the MNET model of Bedeaux and Kjelstrup will be referred to as the "BK-MNET" model in the following.

To compare with the corresponding flux of calcium ions and the reaction rate obtained in the kinetic description, we rewrite the cycle fluxes as

$$\begin{aligned}
J_{\mathrm{a}} &= -\hat{J}_{\mathrm{a}-}\left[1 - \exp\left(\frac{-\Delta_{\mathrm{r}}G}{RT}\right)\right] \\
&\quad + \tilde{J}_{\mathrm{a}-}\left[1 - \exp\left(\frac{\Delta\mu_{\mathrm{Ca/2H}}}{RT}\right)\right], \\
J_{\mathrm{b}} &= -J_{\mathrm{b}-}\left[1 - \exp\left(\frac{-\Delta_{\mathrm{r}}G}{RT}\right)\right], \\
J_{\mathrm{c}} &= \tilde{J}_{\mathrm{c}-}\left[1 - \exp\left(\frac{\Delta\mu_{\mathrm{Ca/2H}}}{RT}\right)\right],
\end{aligned} \tag{34}$$

where $\hat{J}_{a-}$, $\tilde{J}_{a-}$ and $\tilde{J}_{c-}$ are given by

$$\begin{aligned}\hat{J}_{a-} &= J_{a-}\exp\left(\frac{-2\Delta\mu_{Ca/2H}}{RT}\right),\\ \tilde{J}_{a-} &= \hat{J}_{a-}\left[1+\exp\left(\frac{\Delta\mu_{Ca/2H}}{RT}\right)\right],\\ \tilde{J}_{c-} &= J_{c-}\exp\left(\frac{-2\Delta\mu_{Ca/2H}}{RT}\right)\\ &\quad\times\left[1+\exp\left(\frac{\Delta\mu_{Ca/2H}}{RT}\right)\right].\end{aligned} \tag{35}$$

The fluxes are then

$$\begin{aligned}\frac{J_{Ca}}{2} &= -\hat{J}_{a-}\left[1-\exp\left(\frac{-\Delta_r G}{RT}\right)\right]\\ &\quad+(\tilde{J}_{a-}+\tilde{J}_{c-})\left[1-\exp\left(\frac{\Delta\mu_{Ca/2H}}{RT}\right)\right]\end{aligned} \tag{36}$$

and

$$\begin{aligned}r &= -(\hat{J}_{a-}+J_{b-})\left[1-\exp\left(\frac{-\Delta_r G}{RT}\right)\right]\\ &\quad+\tilde{J}_{a-}\left[1-\exp\left(\frac{\Delta\mu_{Ca/2H}}{RT}\right)\right],\end{aligned} \tag{37}$$

which are of the same form as in the BK-MNET model. Comparing the cases when $\Delta\mu_{Ca/2H}=0$, one finds

$$D_{dr}=2J_{a-},\quad D_{rr}=J_{a-}+J_{b-},\quad 2D_{rr}\geq D_{dr}. \tag{38}$$

For the case when $\Delta_r G=0$, one finds

$$D_{dd}/D_{rd}=2(J_{a-}+J_{c-})/J_{a-}\geq 0,\quad D_{dd}\geq 2D_{rd}. \tag{39}$$

Again we find that good estimates can be obtained for D_{ij} through the one-way cycle fluxes J_{j-}, which essentially are equilibrium exchange rates (Kjelstrup et al. 2009)

The mesoscopic description of the fluxes can also be written in the same form by redefining coefficients. In all cases, the resulting flux of calcium ions and the reaction rate are given as exponential functions of the forces (the Gibbs energy of the reaction and the ion exchange) as expected for activated processes.

The BK-MNET model was derived using the reaction coordinate, γ_r, for the ATP reaction and a similar coordinate for the transport of calcium ions, γ_d, as mesoscopic variables. The state of the enzyme is then given by the point (γ_r, γ_d), and the enzyme can be pictured as diffusing in (γ_r, γ_d)-space under a two-dimensional activation energy, $\Phi(\gamma_r,\gamma_d)$. Coupling is introduced by assuming linear force–flux relations on the mesoscopic level, and, on integration over the two mesoscopic coordinates, the relations given in Eq. 33 follow.

Since the states of the enzyme are given by the points in (γ_r, γ_d)-space, we can identify the states in the kinetic cycle description as shown in Table 1, in terms of unknown intermediate points (γ_{dB}, γ_{dD}, γ_{dE}) along the two axes. The cycles can then be pictured as specific paths joining these points, as illustrated in Fig. 7. The mesoscopic variables introduced in the analysis of the cycle correspond to movement along the paths between the different states, for instance $0\leq\gamma_{AB}\leq 1$ is the coordinate corresponding to $0\leq\gamma_d\leq\gamma_{dB}$.

Table 1 The states in the kinetic cycle description as points in (γ_r, γ_d)-space

State	γ_r	γ_d
A	0	0
B	0	γ_{dB}
C	1	γ_{dB}
D	1	γ_{dD}
E	1	γ_{dE}
F	1	1

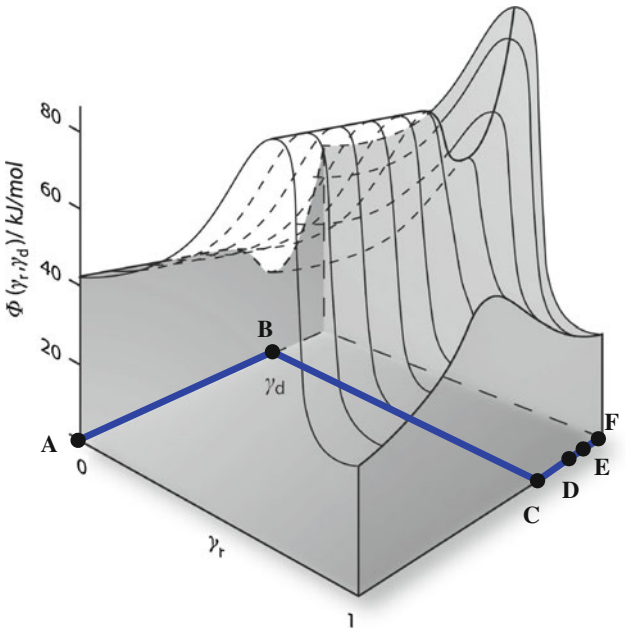

Fig. 7 Illustration of the activation energy landscape of the Ca^{2+}-ATPase with the states and a path corresponding to the projection of cycle a on the (γ_r, γ_d)-plane shown. The path between states A and F is not shown. For cycles b and c, there would also be a path joining states B and D

The BK-MNET model appears less restricted: the enzyme can move along many different paths and pass through many different states [the integration over the coordinates (γ_r, γ_d) can be performed without considering specific paths]. This view is more dynamical in the sense that the enzyme is free to sample the whole configurational space and is not restricted to being in specific states. This opens the possibility for introduction of temperature differences as thermodynamic forces and the corresponding heat fluxes (Kjelstrup et al. 2005b). The probability of following a specific trajectory depends on the activation energy, which is high for the direct transition between

states B and D, meaning that the probability of completing cycles b and c is lower than completing cycle a. Cycle a represents a path where the activation energy is lower, so it will be the dominating cycle of the three.

Conclusions and final remarks

We have analysed the operation of the Ca^{2+}-ATPase ion pump using a kinetic cycle. Using the methodology of Hill, we obtained the cycle fluxes and subsequently the entropy production and the efficiency of the pump. Furthermore, we analysed the cycle using mesoscopic non-equilibrium thermodynamics and showed that the mesoscopic and kinetic approaches result in the same governing equations for the operation of the pump.

Interpretations of Onsager coefficients in terms of unidirectional backward fluxes were found. We propose that these are used in a systematic manner to characterise pumps and motors.

Within the mesoscopic approach, we showed how the activation potentials can be used to identify slow and fast steps of the model. This identification was then used to simplify the model further. Finally, we compared the kinetic and mesoscopic models with the mesoscopic non-equilibrium model of Bedeaux and Kjelstrup and found that the three descriptions are in accordance with each other, but that the latter model is less restricted and can include the temperature differences and the corresponding heat fluxes as additional variables.

Acknowledgments A.L. would like to thank The Faculty of Natural Sciences and Technology, Norwegian University of Science and Technology, for a PhD scholarship.

Appendix: Sum of directional diagrams for the kinetic cycle

For completeness, we show how to obtain the terms in the expression for the sum of the directional diagrams for the complete kinetic cycle, using the methodology of Hill (1989). The first 14 terms are

$$\begin{aligned}\sum = {} & k_{BC}k_{CD}k_{DE}k_{EF}k_{FA} + k_{BA}k_{CD}k_{DE}k_{EF}k_{FA} \\ & + k_{CB}k_{BA}k_{DE}k_{EF}k_{FA} + k_{DC}k_{CB}k_{BA}k_{EF}k_{FA} \\ & + k_{ED}k_{DC}k_{CB}k_{BA}k_{FA} + k_{FE}k_{ED}k_{DC}k_{CB}k_{BA} \\ & + k_{DB}k_{CB}k_{BA}k_{EF}k_{FA} + k_{ED}k_{DB}k_{CB}k_{BA}k_{FA} \\ & + k_{FE}k_{ED}k_{DB}k_{CB}k_{BA} + k_{CB}k_{BD}k_{DE}k_{EF}k_{FA} \\ & + k_{DB}k_{CB}k_{BA}k_{EF}k_{FA} + k_{ED}k_{DB}k_{CB}k_{BA}k_{FA} \\ & + k_{FE}k_{ED}k_{DB}k_{CB}k_{BA} + k_{CB}k_{BD}k_{DE}k_{EF}k_{FA} \\ & + 70\,\text{other terms}. \end{aligned} \quad (40)$$

We consider the kinetic cycle given in Fig. 3 and the sum of directional diagrams of state A. By removing the line connecting states B and D, there are now six ways to remove a second line to create a partial diagram. This gives the first six terms.

By removing the line connecting states D and C, there are four ways to remove a second line to create partial diagrams not already considered. This gives the four next terms.

By removing the line connecting states B and C, there are four ways to remove a second line to create partial diagrams not already considered. This gives the four next terms.

By considering the remaining states in the same fashion, the remaining $5 \times 14 = 70$ terms can be obtained.

References

Alberty RA (2003) Thermodynamics of the hydrolysis of adenosine triphosphate as a function of temperature, pH, pMg, and ionic strength. J Phys Chem B 107:12324–12330

Alberty RA, Goldberg RN (1992) Standard thermodynamic formation properties for the adenosine 5'-triphosphate series. Biochemistry 31:10610–10615

Alonso GL, González DA, Takara D, Ostuni MA, Sánchez GA (2001) Kinetic analysis of a model of the sarcoplasmic reticulum Ca-ATPase, with variable stoichiometry, which enhances the amount and the rate of Ca transport. J Theor Biol 208:251–260

Apell HJ (2004) How do P-Type ATPases transport ions? Bioelectrochemistry 63:149–156

Arruda AP, da Silva WS, Carvalho DP, de Meils L (2003) Hyperthyroidism increases the uncoupled ATPase activity and heat production by the sarcoplasmic reticulum Ca^{2+}-ATPase. Biochem J 375:753–760

Barata H, de Meis L (2002) Uncoupled ATP hydrolysis and thermogenic activity of the sarcoplasmic reticulum Ca^{2+}-ATPase: coupling effects of dimethyl sulfoxide and low temperature. J Biol Chem 277:16868–16872

Bedeaux D, Kjelstrup S (2008) The measurable heat flux that accompanies active transport by Ca^{2+}-ATPase. Phys Chem Chem Phys 10:7304–7317

Berg JM, Tymoczko JL, Stryer L (2002) Biochemistry, 5th edn. W.H. Freeman, New York

de Meis L (2001a) Role of the sarcoplasmic reticulum Ca^{2+}-ATPase on heat production and thermogenesis. Biosci Rep 21:113–137

de Meis L (2001b) Uncoupled ATPase activity and heat production by the sarcoplasmic reticulum Ca^{2+}-ATPase. J Biol Chem 276:25078–25087

de Meis L (2002) Ca^{2+}-ATPases (SERCA): energy transduction and heat production in transport ATPases. J Membrane Biol 188:1–9

de Meis L (2003) Brown adipose tissue Ca^{2+}-ATPase uncoupled ATP hydrolysis and thermogenic activity. J Biol Chem 278:41856–41861

de Meis L, Bianconi ML, Suzano VA (1997) Control of energy fluxes by the sarcoplasmic reticulum Ca^{2+}-ATPase: ATP hydrolysis, ATP synthesis and heat production. FEBS Lett 406:201–204

de Meis L, Oliveira GM, Arruda AP, Santos R, da Costa RM, Benchimol M (2005) The thermogenic activity of rat brown

adipose tissue and rabbit white muscle Ca^{2+}-ATPase. IUBMB Life 57:337–345

Froud RJ, Lee AG (1986) A model for the phosphorylation of the Ca^{2+} + Mg^{2+}-activated ATPase by phosphate. Biochem J 237:207–215

Garrett RH, Grisham CM (2010) Biochemistry, 4th edn. Brooks Cole, Boston

Gould GW, East JM, Froud RJ, McWhirter JM, Stefanova HI, Lee AG (1986) A kinetic model for the Ca^{2+} + Mg^{2+}-activated ATPase of sarcoplasmic reticulum. Biochem J 237:217–227

Hasselbach W, Makinose M (1961) Die Calciumpumpe der "Erschlaffungsgrana" des Muskels und ihre Abhängigkeit von der ATP-Spaltung. Biochem Z 333:518–528

Haynes DH, Mandveno A (1987) Computer modeling of Ca^{2+} pump function of Ca^{2+} − Mg^{2+}-ATPase of sarcoplasmic reticulum. Physiol Rev 67:244–284

Hill TL (1982) The linear Onsager coefficients for biochemical kinetic diagrams as equilibrium one-way cycle fluxes. Nature 299:84–86

Hill TL (1989) Free energy transduction and biochemical cycle kinetics. Springer, New York

Jensen AML, Sørensen TLM, Olesen C, Møller JV, Nissen P (2006) Modulatory and catalytic modes of ATP binding by the calcium pump. EMBO J 25:2305–2314

Kanazawa T, Yamada S, Yamamoto T, Tonomura Y (1971) Reaction mechanism of the Ca^{2+}-dependent ATPase of sarcoplasmic reticulum from skeletal muscle: V. vectorial requirements for calcium and magnesium ions of three partial reactions of ATPase: formation and decomposition of a phosphorylated intermediate and ATP-formation from ADP and the intermediate. J Biochem (Tokyo) 70:95–123

Kjelstrup S, Bedeaux D (2008) Non-equilibrium thermodynamics of heterogeneous systems. World Scientific, Singapore

Kjelstrup S, Rubi JM, Bedeaux D (2005) Active transport: a kinetic description based on thermodynamic grounds. J Theor Biol 234:7–12

Kjelstrup S, Rubi JM, Bedeaux D (2005) Energy dissipation in slipping biological pumps. Phys Chem Chem Phys 7:4009–4018

Kjelstrup S, de Meis L, Bedeaux D, Simon JM (2008) Is the Ca^{2+}-ATPase from sarcoplasmic reticulum also a heat pump? Eur Biophys J 38:59–67

Kjelstrup S, Barragán D, Bedeaux D (2009) Coefficients for active transport and thermogenesis of Ca^{2+}-ATPase isoforms. Biophys J 96:4368–4376

Kjelstrup S, Bedeaux D, Johannessen E, Gross J (2010) Non-equilibrium thermodynamics for engineers. World Scientific, Singapore

Kodama T, Kurebayashi N, Harafuji H, Ogawa Y (1982) Calorimetric evidence for large entropy changes accompanying intermediate steps of the ATP-driven Ca^{2+} uptake by sarcoplasmic reticulum. J Biol Chem 257:4238–4241

Kühlbrandt W (2004) Biology, structure and mechanism of P-type ATPases. Nat Rev Mol Cell Biol 5:282–295

Laursen M, Bublitz M, Moncoq K, Olesen C, Møller JV, Young HS, Nissen P, Morth JP (2009) Cyclopiazonic acid is complexed to a divalent metal ion when bound to the sarcoplasmic reticulum Ca^{2+}-ATPase. J Biol Chem 284:13513–13518

Lee AG, East JM (2001) What the structure of a calcium pump tells us about its mechanism. Biochem J 356:665–683

Mahmmoud YA (2008) Capsaicin stimulates uncoupled ATP hydrolysis by the sarcoplasmic reticulum calcium pump. J Biol Chem 283:21418–21426

Mall S, Broadbridge R, Harrison SL, Gore MG, Lee AG, East JM (2006) The presence of sarcolipin results in increased heat production by Ca^{2+}-ATPase. J Biol Chem 281:36597–36602

McWhirter JM, Gould GW, East JM, Lee AG (1987) A kinetic model for Ca^{2+} efflux mediated by the Ca^{2+} + Mg^{2+}-activated ATPase of sarcoplasmic reticulum. Biochem J 245:713–721

Mintz E, Guillain F (1997) Ca^{2+} transport by the sarcoplasmic reticulum ATPase. Biochim Biophys Acta 1318:52–70

Møller JV, Olesen C, Winther AML, Nissen P (2010) The sarcoplasmic Ca^{2+}-ATPase: design of a perfect chemi-osmotic pump. Q Rev Biophys 43:501–566

Moncoq K, Trieber CA, Young HS (2007) The molecular basis for cyclopiazonic acid inhibition of the sarcoplasmic reticulum calcium pump. J Biol Chem 282:9748–9757

Nelson P (2003) Biological physics: energy, information, life. W.H. Freeman, New York

Obara K, Miyashita N, Xu C, Toyoshima I, Sugita Y, Inesi G, Toyoshima C (2005) Structural role of countertransport revealed in Ca^{2+} pump crystal structure in the absence of Ca^{2+}. Proc Natl Acad Sci USA 102:14489–14496

Olesen C, Sørensen TLM, Nielsen RC, Møller JV, Nissen P (2004) Dephosphorylation of the calcium pump coupled to counterion occlusion. Science 306:2251–2255

Olesen C, Picard M, Winther AML, Gyrup C, Morth JP, Oxvig C, Møller JV, Nissen P (2007) The structural basis of calcium transport by the calcium pump. Nature 450:1036–1042

Olesen C, Picard M, Winther AML, Gyrup C, Morth JP, Oxvig C, Møller JV, Nissen P (2007) The structural basis of calcium transport by the calcium pump. Nature 450:1036–1042

Peinelt C, Apell HJ (2004) Time-resolved charge movements in the sarcoplasmatic reticulum Ca-ATPase. Biophys J 86:815–824

Peinelt C, Apell HJ (2005) Kinetics of Ca^{2+} binding to the SR Ca-ATPase in the E_1 state. Biophys J 89:2427–2433

Qian H (2005) Cycle kinetics, steady state thermodynamics and motors-a paradigm for living matter physics. J Phys Condens Matter 17:S3783–S3794

Qian H (2007) Phosphorylation energy hypothesis: open chemical systems and their biological functions. Annu Rev Phys Chem 58:42–113

Qian H (2009) Entropy demystified the "thermo"-dynamics of stochastically fluctuating systems. Methods Enzymol 467:34–111

Qian M, Zhang X, Wilson RJ, Feng J (2008) Efficiency of Brownian motors in terms of entropy production rate. EPL (Europhys Lett) 84(1):10014

Schatzmann HJ (1966) ATP-dependent Ca^{++}-Extrusion from human red cells. Experientia 22:364–365

Smith NP, Crampin EJ (2004) Development of models of active ion transport for whole-cell modelling: cardiac sodium–potassium pump as a case study. Prog Biophys Mol Biol 85:387–405

Søhoel H, Jensen AML, Møller JV, Nissen P, Denmeade SR, Isaacs JT, Olsen CE, Christensen SB (2006) Natural products as starting materials for development of second-generation SERCA inhibitors targeted towards prostate cancer cells. Bioorg Med Chem 14:2810–2815

Sørensen TLM, Møller JV, Nissen P (2004) Phosphoryl transfer and calcium ion occlusion in the calcium pump. Science 304: 1672–1675

Takahashi M, Kondou Y, Toyoshima C (2007) Interdomain communication in calcium pump as revealed in the crystal structures with transmembrane inhibitors. Proc Natl Acad Sci USA 104:5800–5805

Toyoshima C, Mizutani T (2004) Crystal structure of the calcium pump with a bound ATP analogue. Nature 430:529–535

Toyoshima C, Nomura H (2002) Structural changes in the calcium pump accompanying the dissociation of calcium. Nature 418:605–611

Toyoshima C, Nakasako M, Nomura H, Ogawa H (2000) Crystal structure of the calcium pump of sarcoplasmic reticulum at 2.6 Å resolution. Nature 405:647–655

Toyoshima C, Nomura H, Tsuda T (2004) Lumenal gating mechanism revealed in calcium pump crystal structures with phosphate analogues. Nature 432:361–368

Toyoshima C, Norimatsu Y, Iwasawa S, Tsuda T, Ogawa H (2007) How processing of aspartylphosphate is coupled to lumenal gating of the ion pathway in the calcium pump. Proc Natl Acad Sci USA 104:19831–19836

Toyoshima C, Yonekura SI, Tsueda J, Iwasawa S (2011) Trinitrophenyl derivatives bind differently from parent adenine nucleotides to Ca^{2+}-ATPase in the absence of Ca^{2+}. Proc Natl Acad Sci USA 108:1833–1838

Tran K, Smith NP, Loiselle DS, Crampin EJ (2009) A thermodynamic model of the cardiac sarcoplasmic/endoplasmic Ca^{2+} (SERCA) pump. Biophys J 96:2029–2042

Winther AML, Liu H, Sonntag Y, Olesen C, le Maire M, Soehoel H, Olsen CE, Christensen SB, Nissen P, Møller JV (2010) Critical roles of hydrophobicity and orientation of side chains for inactivation of sarcoplasmic reticulum Ca^{2+}-ATPase with thapsigargin and thapsigargin analogs. J Biol Chem 285:28883–28892

Xu C, Rice WJ, He W, Stokes DL (2002) A structural model for the catalytic cycle of Ca^{2+}-ATPase. J Mol Biol 316:201–211